6th International Conference on Computational and Mathematical Biomedical Engineering – CMBE2019
10-12 June 2019, Japan
P. Nithiarasu, M. Ohta, M. Oshima (Eds.)

HOW BIOMECHANICAL PROPERTIES OF RED BLOOD CELLS CHANGE WITH TEMPERATURE

A.S. Ademiloye
Zienkiewicz Centre for Computational Engineering, College of Engineering,
Swansea University, Bay Campus, Swansea SA1 8EN, United Kingdom, a.s.ademiloye@swansea.ac.uk

SUMMARY

In recent decades, the biomechanical properties of human red blood cells (RBCs) have been greatly explored by numerous researchers for diverse reasons. In normal physiological conditions, RBCs undergoes large deformation when traversing thin microcapillaries, however, upon infection by different blood-related diseases such as malaria, they experience impaired deformability. This paper examines how biomechanical properties of RBCs change with temperature using a multiscale meshfree method. The multiscale meshfree method offers improved accuracy and better computational efficiency as it incorporates RBC membrane microstructural configuration into its constitutive formulation, thereby providing better insights into the changes on the atomistic level.

Keywords: *Red blood cell, biomechanical properties, multiscale meshfree method*

1 INTRODUCTION

Red blood cells (RBCs) alone account for more than 99% of the particulate matter in blood and about 40–45% of the blood by volume. Mature RBCs are non-nucleated and highly differentiated biconcave cells that consist of a lipid bilayer with an attached spectrin network and an inner fluid (cytosol) with dissociated protein hemoglobin. RBC diameter and membrane thickness are about 8 μm and 10 nm, respectively. The biomechanical properties and biorheological behaviors of RBC membrane are very essential for sustaining cell functions and they have strong links to the overall state of human well-being since changes in these properties may eventually lead to the manifestation of various blood related hereditary and non-hereditary diseases.

According to the World Malaria Report 2015 published by the World Health Organization (WHO), malaria can be described as the most important parasitic and non-hereditary blood disease of humans as it claims the lives of more children worldwide than any other infectious disease. In the year 2015 alone, around 214 million new cases of malaria infection and ~438,000 malaria deaths occurred worldwide [1]. Of all the known malaria parasites, *Plasmodium falciparum (P. falciparum)*, which is a protozoan parasite transmitted through the bite of infected female Anopheles mosquito, has been identified as the most prevalent and lethal malaria parasite affecting humans [2,3]. Generally, the merozoites develop through the ring (*Pf*-rRBC), trophozoite (*Pf*-tRBC) and schizont (*Pf*-sRBC) stages with varying properties and degrees of influence on the cell properties. Trophozoite (*Pf*-tRBC) stage has been identified as the most active stage of malaria development. The product of this dynamic invasion process is the bursting of the RBCs resulting in anemia, chills, and fever [4]. Other notable effects of infection include increased membrane shear modulus, cell viscosity and cytoadherence [5].

Noteworthy numerical studies into the effect of malaria infection on RBC membrane include the works by Dupin et al. [6] using a 3D lattice Boltzmann model, Hosseini and Feng [7] by means of smoothed particle hydrodynamics (SPH) method and dissipative particle dynamics (DPD) method by Fedosov et al. [8]. In a bid to predict the large deformation behaviors of the iRBC membrane more precisely and elucidate their stiffening mechanism, a nonlinear 3D multiscale RBC membrane model is proposed in this study. The developed 3D multiscale RBC multiscale model, based on the 2D atomistic-continuum model presented in Ref. [9], is computationally efficient and able to

capture the atomistic scale behavior of RBC membrane more accurately. This approach has been successfully applied to study the biomechanical behavior of healthy RBC membrane [10,11].

2 MULTISCALE MESHFREE COMPUTATIONAL FRAMEWORK

2.1 Multiscale hyperelastic constitutive model

In this section, we describe the development of a hyperelastic constitutive model that is derived from the first-order Cauchy–Born rule by using the coarse-grained Helmholtz free energy to describe the membrane atomic interactions. The Cauchy–Born rule establishes a connection between the deformation of the lattice vector of an atomistic system and that of a continuum displacement field and plays an important role in the development of continuum constitutive models of atomic lattices. Considering a representative microstructure that is composed of six spectrin links $I-J(J=1,\ldots,6)$ as shown in Fig. 1, the deformation of each spectrin links can be approximated using the Cauchy–Born rule, as follows,

$$\boldsymbol{r}_{IJ} = \boldsymbol{Grad} \otimes \boldsymbol{R}_{IJ}, \tag{1}$$

where $\boldsymbol{Grad} = Grad_{iJ} e_i \otimes e_J$, $\boldsymbol{R}_{IJ}$ and $\boldsymbol{r}_{IJ}$ denotes the first-order deformation gradient tensor, the undeformed and deformed spectrin link length between junction complexes *I* and *J*, respectively.

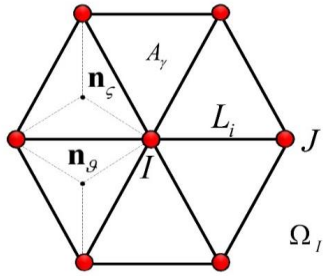

Figure 1: Representative microstructure of the RBC membrane

In our current derivation, the strain energy density function W_0 at a junction complex *I* of the RBC membrane representative microstructure is defined using the coarse-grained Helmholtz free energy at this point, which is obtained as a summation of membrane in-plane and bending energies, and expressed as

$$W_0 = W_0(\boldsymbol{Grad}) = \frac{h}{\Omega_I}\left[\frac{1}{2}\sum_{J=1}^{6} U_{WLC}(\boldsymbol{r}_{IJ}) + \frac{1}{3}\sum_{\gamma=1}^{6} C/\boldsymbol{A}_\gamma + U_{Bending}(\theta_{\psi\varphi})\right], \tag{2}$$

where h represents RBC membrane thickness and Ω_I is the average area per junction complex in the reference configuration, calculated using $\sqrt{3}L_i^{\,2}/2$. The terms in Eq. (2) can be expressed as

$$U_{WLC}(\boldsymbol{r}_{IJ}) = \frac{k_B T L_{\max}}{4p}\cdot\frac{(3x_0^2 - 2x_0^3)}{1-x_0}, \quad C = \frac{3\sqrt{3}k_B T L_{\max}^3 x_0^4\ \ 4x_0^2 - 9x_0 + 6}{64p\ \ 1-x_0^{\ 2}},$$
$$U_{Bending}(\theta_{\psi\varphi}) = \bar{k}_b \sum_{\langle\psi,\varphi\rangle=1}^{3} [1-\cos(\theta_{\psi\varphi} - \theta_0)] \tag{3}$$

where $x_0 = L_{\max}/L$, p, $L_{\max}$, k_B, $\boldsymbol{A}_\gamma$, and T, respectively, denote the persistence length, the maximum spectrin extension length, the Boltzmann constant, given as 1.38×10^{-23} JK^{-1}, area of each triangular plaquette in the unit cell, and the physiological temperature, which was varied from subzero to above-room temperature values to examine the influence of temperature on RBC membrane deformability. The terms $\theta_{\psi\varphi}$ and θ_0 (= 0), respectively, denote the instantaneous and spontaneous curvature angles between two neighboring triangles as illustrated in Fig. 1. The first-order Piola-Kirchhoff stress tensor $\boldsymbol{P}$ and the tangent modulus matrix $\boldsymbol{M}$ corresponding to the

first- and second-order derivative of the strain energy density with respect to $\boldsymbol{Grad}$, respectively can be calculated using,

$$\boldsymbol{P} = \frac{\partial W_0}{\partial \boldsymbol{Grad}} = \left[\frac{\partial \boldsymbol{r}_{IJ}}{\partial \boldsymbol{Grad}}\right] \cdot \left[\frac{\partial W_0}{\partial \boldsymbol{r}_{IJ}}\right] \text{ and } \boldsymbol{M} = \frac{\partial^2 W_0}{\partial \boldsymbol{Grad}^2} = \left[\frac{\partial \boldsymbol{r}_{IJ}}{\partial \boldsymbol{Grad}}\right] \cdot \left[\frac{\partial^2 W_0}{\partial \boldsymbol{r}_{IJ}^{\,2}}\right] \cdot \left[\frac{\partial \boldsymbol{r}_{IJ}}{\partial \boldsymbol{Grad}}\right]^T. \quad (4)$$

2.2 Nonlinear meshfree computational framework

A nonlinear three-dimensional (3D) multiscale meshfree method based on the improved moving least-squares (IMLS) approximation and Ritz minimization scheme, is employed to investigate the effect of malaria infection on the large deformation behavior of iRBC membrane. The current approach is well able to overcome the inherent limitations of mesh-based methods since it satisfies the higher order continuity requirements, circumvent mesh distortion, increased computation cost due to remeshing process and owing to the nonlocal intrinsic properties of meshfree methods, displacements are the only nodal degree of freedom [12]. We refer readers who are interested in the derivation and numerical computation procedure of the expressions in (1)–(4) above as well as the meshfree development and implementation to the following literature and the references cited therein [9,13–15].

Table I Values of microstructure parameters for healthy RBC and iRBC membrane

Cell condition / infection stage	RBC membrane microstructure parameters			
	Equilibrium spectrin length, L (nm)	Persistence length, p (nm)	Maximum contour length, L_{max} (nm)	RBC diameter (μm)
hRBC	87.0	8.5	238	7.820
Pf-tRBC	139.2	6.0	238	7.260

2.3 Numerical simulation procedure

The full biconcave geometry of the RBC membrane was used for all numerical simulations in this study since the precise shapes of the various infection stages are unknown. This geometry was first discretized with meshfree nodes. Stretching forces ranging from 0 – 195 pN was applied to the ends of the cell and pulled. These simulations were performed using an in-house MATLAB code. The variation of the elongation index, EI of hRBC and *Pf*-tRBC membrane, computed with RBC deformed axial d_a and transverse d_t diameters using EI = $(d_a - d_a)/(d_a + d_a)$ as temperature changes were plotted against increasing stretching force. The sets of RBC membrane microstructure parameters presented in Table I are dependent on the condition of the cell membrane. Other simulation parameters are defined irrespective of the RBC condition. They include the membrane thickness, h = 12 nm and the RBC membrane bending coefficient, $\bar{k}_b = 2.77 \times 10^{-19}$ J. Results obtained from our numerical simulations have been compared and validated against experimental results reported in Ref. [16].

3 RESULTS AND CONCLUSIONS

Figure 2 shows the effects of varying temperature from the subzero to above room temperature regions for hRBC and *Pf*-tRBC infection stage. It was observed that the effect of temperature change is nearly negligible in the small deformation region when applied stretching force is between 0 and 50pN since the elongation index curves for various temperature values are nearly linear and very close. Beyond this applied stretching force range, the influence of temperature increment on the deformability of iRBC membrane becomes more obvious and the degree of nonlinearity and curvature of the elongation index polynomic curves reduces as the parasitic infection progresses. This suggests that as the malaria infection progresses, the overall rigidity of the iRBC membrane grows, primarily due to the remodeling and microstructural changes as well as possible denaturation of the membrane underlying spectrin protein network owing to the disruption and destruction of the spectrin cytoskeleton secondary and tertiary protein structure as a result of thermal treatments. These changes lead to an overall decrease in RBC membrane deformability.

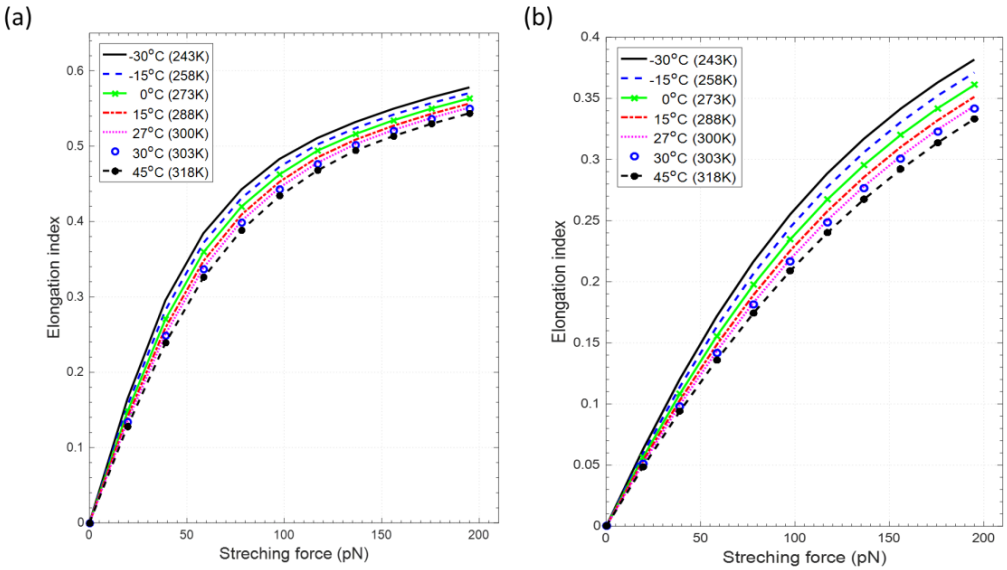

Figure 2: Measurement of membrane deformability using the variation of elongation index as a function of applied stretching forces as temperature changes for (a) healthy RBCs and (b) *Pf*-tRBCs.

ACKNOWLEDGEMENT

The author gratefully appreciates the support provided by Zienkiewicz Centre for Computational Engineering, College of Engineering, Swansea University, Swansea, United Kingdom.

REFERENCES

[1] W.H. Organization, World malaria report 2015, Geneva WHO. (2015).

[2] I.J. Udeinya, J.A. Schmidt, M. Aikawa, L.H. Miller, I. Green, Falciparum malaria infected erythrocytes specifically bind to cultured human endothelial cells., Science (80-.). 213 (1981) 555–557.

[3] Malaria | pathology | Britannica.com, (n.d.). https://www.britannica.com/science/malaria#ref241509 (accessed December 3, 2018).

[4] G.D. Schmidt, L.S. Roberts, J. Janovy, Foundations of parasitology, 8th ed., New York, 2009.

[5] A.F. Cowman, D. Berry, J. Baum, The cellular and molecular basis for malaria parasite invasion of the human red blood cell., J. Cell Biol. 198 (2012) 961–71. doi:10.1083/jcb.201206112.

[6] M.M. Dupin, I. Halliday, C.M. Care, L.L. Munn, Lattice Boltzmann modelling of blood cell dynamics, Int. J. Comut. Fluid Dyn. 22 (2008) 481–492. doi:10.1080/10618560802238242.

[7] S.M. Hosseini, J.J. Feng, How malaria parasites reduce the deformability of infected red blood cells., Biophys. J. 103 (2012) 1–10. doi:10.1016/j.bpj.2012.05.026.

[8] D.A. Fedosov, B. Caswell, G.E. Karniadakis, Systematic coarse-graining of spectrin-level red blood cell models, Comput. Methods Appl. Mech. Eng. 199 (2010) 1937–1948. doi:10.1016/j.cma.2010.02.001.

[9] A.S. Ademiloye, L.W. Zhang, K.M. Liew, Numerical computation of the elastic and mechanical properties of red blood cell membrane using the higher-order Cauchy–Born rule, Appl. Math. Comput. 268 (2015) 334–353. doi:10.1016/j.amc.2015.06.071.

[10] A.S. Ademiloye, L.W. Zhang, K.M. Liew, A multiscale framework for large deformation modeling of RBC membranes, Comput. Methods Appl. Mech. Eng. 329 (2018) 144–167. doi:10.1016/j.cma.2017.10.004.

[11] A.S. Ademiloye, L.W. Zhang, K.M. Liew, Atomistic–continuum model for probing the biomechanical properties of human erythrocyte membrane under extreme conditions, Comput. Methods Appl. Mech. Eng. 325 (2017) 22–36. doi:10.1016/j.cma.2017.06.033.

[12] L.W. Zhang, A.S. Ademiloye, K.M. Liew, Meshfree and Particle Methods in Biomechanics: Prospects and Challenges, Arch. Comput. Methods Eng. 2 (2018). doi:10.1007/s11831-018-9283-2.

[13] A.S. Ademiloye, L.W. Zhang, K.M. Liew, Predicting the elastic properties and deformability of red blood cell membrane using an atomistic-continuum approach, in: D.D. Feng, A.M. Korsunsky, S.I. Ao, C. Douglas, O. Castillo (Eds.), Proc. Int. MultiConference Eng. Comput. Sci. 2016, Newswood Limited, Hong Kong, 2016: pp. 942–946. doi:10.13140/RG.2.1.3088.8082.

[14] X.Y. Wang, X. Guo, Z. Su, A quasi-continuum model for human erythrocyte membrane based on the higher order Cauchy–Born rule, Comput. Methods Appl. Mech. Eng. 268 (2014) 284–298. doi:10.1016/j.cma.2013.08.020.

[15] L.W. Zhang, A.S. Ademiloye, K.M. Liew, A multiscale Cauchy-Born meshfree model for deformability of red blood cells parasitized by Plasmodium falciparum, J. Mech. Phys. Solids. 101 (2017) 268–284. doi:10.1016/j.jmps.2017.01.009.

[16] S. Suresh, J. Spatz, J.P. Mills, A. Micoulet, M. Dao, C.T. Lim, M. Beil, T. Seufferlein, Connections between single-cell biomechanics and human disease states: Gastrointestinal cancer and malaria, Acta Biomater. 1 (2005) 15–30. doi:10.1016/j.actbio.2015.07.015.